

US-FT/7-95

BEAUTY HADRON PRODUCTION AT HERA-B ENERGY IN DUAL PARTON MODELS

N. Armesto, C. Pajares and Yu. M. Shabelski*

*Departamento de Física de Partículas, Universidade de Santiago de Compostela,
15706-Santiago de Compostela, Spain*

ABSTRACT

Production of charmed and beauty mesons and baryons in hadron–nucleon collisions at not very high energy is considered in the framework of the Quark–Gluon String Model. We take into account the possible corrections to the model which disappear at asymptotically high energies but could be important at comparatively low energies, essentially in the case of heavy flavour production. The case of nuclear targets is also considered and the A –dependence of charmed and beauty hadron yields is calculated. Predictions for the case of beauty hadron production at $\sqrt{s} = 39$ GeV are presented.

*Permanent address: Leningrad Nuclear Physics Institute, Gatchina, Sanct–Petersburg 188350, USSR.

May 1995
US-FT/7-95

1. INTRODUCTION

Heavy flavour production processes at high energies are considered usually in the framework of QCD, see e.g. [1–3], which allows one to describe quantitatively the cross sections of c , b and t quark production, their dependence on the transverse momentum of the heavy quark, the rapidity distributions, etc. However, these approaches do not allow to calculate the spectra of different mesons and baryons. In the case of high energies there is also the problem of the parton structure function behaviour in the very small x region whereas at comparatively small energies the results depend significantly on the values of the heavy quark mass and the QCD scale (see e.g. [4,5]).

Another approach to heavy flavour production processes has been considered in Ref. [6] in the framework of the Quark–Gluon String Model (QGSM). This model is a version of the Dual Topological Unitarization (DTU) and describes quite reasonably many features of high energy production processes, including the inclusive spectra of different secondary hadrons, their multiplicities, KNO-distributions, etc., both in hadron–nucleon and hadron–nucleus collisions [7–10]. High energy interactions are considered as proceeding via the exchange of one or several pomerons and all elastic and inelastic processes result from cutting pomerons or between pomerons [11]. The possibility of exchanging a different number of pomerons introduces absorptive corrections to the inclusive cross sections which are in agreement with the experimental data on production of hadrons consisting in light quarks. The inclusive spectrum of heavy flavoured hadrons in QGSM was considered earlier in Refs. [6,12,13].

In the present paper we discuss the possibility of using QGSM for calculating heavy flavour production at not very high energies. If the ratio m_h/\sqrt{s} is not negligibly small some corrections can appear, which disappear with increasing energy. We consider several variants of such corrections and compare the results with the experimental data on charm and beauty production by proton and pion beams. These corrections can also change the predicted A -dependence of charm and beauty production. In particular we present quantitative predictions for B -meson and Λ_b production by protons on nucleon and tungsten targets at HERA–B [14] energy, which we assume to be equal $\sqrt{s} = 39$ GeV (i.e., $p_{lab} \approx 800$ GeV/c).

We also present the results on beauty production at HERA–B energy obtained with a QGSM-based Monte Carlo code in which each inelastic collision is considered as a hard gluon–gluon one, simulated by PYTHIA. The A -dependence of beauty production in hadron–nucleus collisions obtained in this case is very different from two of the three variants of the low energy corrections considered in the analytical calculations.

2. INCLUSIVE SPECTRA OF HEAVY FLAVOURED HADRONS IN QGSM

As mentioned above high energy hadron–nucleon and hadron–nucleus interactions are

considered in the QGSM as proceeding via the exchange of one or several pomerons. Each pomeron corresponds to a cylindrical diagram so in the case of cutting a pomeron two showers of secondaries are produced, see Fig. 1. The inclusive spectrum of secondaries is determined by the convolution of diquark, valence and sea quark distributions $u(x, n)$ in the incident particles and the fragmentation functions $G(z)$ of quarks and diquarks into secondary hadrons. The diquark and quark distribution functions depend on the number n of cut pomerons in the considered diagram. In the case of a nucleon target the inclusive spectrum of a secondary hadron h has the form [7]:

$$1/\sigma_{inel} d\sigma/dx = \sum_{n=1}^{\infty} w_n \phi_n^h(x) , \quad (1)$$

where the functions $\phi_n^h(x)$ determine the contribution of diagrams with n cut pomerons and w_n is the probability of this process. Here we neglect the contributions of diffraction dissociation processes which are comparatively small in the case of charmed and beauty hadron production.

For pp collisions

$$\phi_n^h(x) = f_{qq}^h(x_+, n) f_q^h(x_-, n) + f_q^h(x_+, n) f_{qq}^h(x_-, n) + 2(n-1) f_s^h(x_+, n) f_s^h(x_-, n) , \quad (2)$$

$$x_{\pm} = \frac{1}{2} [\sqrt{4m_T^2/s + x^2} \pm x] , \quad (3)$$

where f_{qq} , f_q and f_s correspond to the contributions of diquarks, valence and sea quarks respectively. They are determined by the convolution of the diquark and quark distributions with the fragmentation functions, e.g.,

$$f_q^h(x_+, n) = \int_{x_+}^1 u_q(x_1, n) G_q^h(x_+/x_1) dx_1 . \quad (4)$$

In the case of a meson beam the diquark contributions in Eq. (2) should be changed by the contribution of valence antiquarks. The diquark and quark distributions as well as the fragmentation functions are determined via their Regge asymptotics with accounting for conservation laws [7,9].

In present calculations we use quark and diquark distributions in the proton of the form [7]:

$$u_{uu}(x, n) = C_{uu} x^{2.5} (1-x)^{n-1.5} , \quad (5)$$

$$u_{ud}(x, n) = C_{ud} x^{1.5} (1-x)^{n-1.5} , \quad (6)$$

$$u_u(x, n) = C_u x^{-0.5} (1-x)^{n+0.5} , \quad (7)$$

$$u_d(x, n) = C_d x^{-0.5} (1-x)^{n+1.5} , \quad (8)$$

$$u_{\bar{u}}(x, n) = u_{\bar{d}}(x, n) = C_{\bar{u}} x^{-0.5} [(1+\delta/2) \times (1-x)^{n+0.5} (1-x/3) - \delta/2 (1-x)^{n+1}] , \quad n > 1 , \quad (9)$$

$$u_s(x, n) = C_s x^{-0.5} (1-x)^{n+1} , \quad n > 1 , \quad (10)$$

where $\delta = 0.2$ is the relative probability to find a strange quark in the sea. The factors C_i are determined from the normalization condition

$$\int_0^1 u_i(x, n) dx = 1 . \quad (11)$$

The fragmentation functions of quarks and diquarks into charmed mesons and baryons were changed a little in comparison with Ref. [12] to obtain a better agreement with the existing experimental data. We use these functions in the form

$$G_u^{\overline{D^0}} = G_d^{D^-} = a_0(1-z)^{\lambda-\alpha_\psi(0)}(1+a_1z^2) , \quad (12)$$

$$G_u^{D^-} = G_u^{D^+} = G_u^{D^0} = G_d^{D^+} = G_d^{D^0} = G_d^{\overline{D^0}} = a_0(1-z)^{1+\lambda-\alpha_\psi(0)} , \quad (13)$$

$$G_{uu}^{D^+} = G_{uu}^{D^-} = G_{uu}^{D^0} = G_{ud}^{D^+} = G_{ud}^{D^0} = a_0(1-z)^{3+\lambda-\alpha_\psi(0)} , \quad (14)$$

$$G_{uu}^{\overline{D^0}} = a_0(1-z)^{2+\lambda-\alpha_\psi(0)}(1+a_2z^2) , \quad (15)$$

$$G_{ud}^{\overline{D^0}} = a_0(1-z)^{2+\lambda-\alpha_\psi(0)}(1-z+a_2z^2/2) , \quad (16)$$

$$G_{uu}^{\Lambda_c} = G_{ud}^{\Lambda_c} = a_{01}(1-z)^{6+\lambda-\alpha_\psi(0)} , \quad (17)$$

$$G_u^{\Lambda_c} = G_d^{\Lambda_c} = a_{01}(1-z)^{2+\lambda-\alpha_\psi(0)} , \quad (18)$$

$$G_{\overline{u}}^{\Lambda_c} = G_{\overline{d}}^{\Lambda_c} = G_u^{\Lambda_c}(1-z) . \quad (19)$$

In the case of Λ_c production there are two different contributions [8]. The first one corresponds to the central production of a $\Lambda_c\overline{\Lambda}_c$ pair and can be described by the previous formulas. The second contribution is connected with the direct fragmentation of the initial baryon into Λ_c with conservation of the string junction. To account for this possibility we input into Eq. (2), instead of $f_q(x_+, n)$ and $f_q(x_-, n)$, two additional items $f_{qq2}(x_+, n)$ and $f_{qq2}(x_-, n)$ multiplied by $(1-x_-)^{-\alpha_\psi(0)}$ and $(1-x_+)^{-\alpha_\psi(0)}$ respectively. The values of $f_{qq2}(x_+, n)$ and $f_{qq2}(x_-, n)$ are determined by the corresponding fragmentation functions

$$G_{uu2}^{\Lambda_c} = a_{02}z^2(1-z)^{1+\lambda-\alpha_\psi(0)} , \quad (20)$$

$$G_{ud2}^{\Lambda_c} = a_{02}z^2(1-z)^{\lambda-\alpha_\psi(0)} . \quad (21)$$

The probability for a process to have n cutted pomerons was calculated using the quasieikonal approximation [7,15]:

$$w_n = \sigma_n / \sum_{n=1}^{\infty} \sigma_n , \quad \sigma_n = \frac{\sigma_P}{nz} \left(1 - e^{-z} \sum_{k=0}^{n-1} \frac{z^k}{k!}\right) , \quad (22)$$

$$z = \frac{2C\gamma}{R^2 + \alpha'\xi} e^{\Delta\xi} , \quad \sigma_P = 8\pi\gamma e^{\Delta\xi} , \quad \xi = \ln(s/1 \text{ GeV}^2) , \quad (23)$$

with parameters

$$\Delta = 0.139, \alpha' = 0.21 \text{ GeV}^{-2}, \gamma_{pp} = 1.77, \gamma_{\pi p} = 1.07, \\ R_{pp}^2 = 3.18 \text{ GeV}^{-2}, R_{\pi p}^2 = 2.48 \text{ GeV}^{-2}, C_{pp} = 1.5, C_{\pi p} = 1.65.$$

In the case of secondary production at not very high energy or if the mass of the secondary hadron is comparatively large some problems appear in QGSM. Their origin is connected with the normalization (to unity) of quark and diquark distributions. The probability for any quark or diquark to fragment into a secondary hadron h is also normalized to unity,

$$\sum_h \int_0^1 G_i^h(z) G_i^h(0) dz = 1. \quad (24)$$

However the lower limit of integration in Eq. (4) is higher than zero. The minimal value of x_1 is $x_{1min} \approx m_T^2/s$, so the quark having $x_1 < x_{1min}$ cannot fragment into a secondary hadron. As a result the sum of the energy of all secondaries becomes slightly smaller than the initial energy. The problem is more clear in the case of a quark which exists in the initial hadron. For example in the case of Dp collisions at not very high energy the multiplicity of secondary charmed hadrons will be smaller than unity. QGSM is based on the Regge theory which contains many other corrections of the same order m_h^2/s which have been omitted. However even numerically a small nonconservation of energy and quantum numbers can produce problems. To avoid them we consider two possibilities to correct QGSM. The simplest way is to use the normalization condition

$$\int_{m_T^2/s}^1 u_i(x, n) dx = 1 \quad (25)$$

instead of Eq. (11). Another possibility is to multiply every f_i in Eq. (2) by a factor

$$D_n^+ = \int_0^1 f_i^h(x, n) dx / \int_0^1 f_i^h(x_+, n) dx \quad (26)$$

and

$$D_n^- = \int_{-1}^0 f_i^h(x, n) dx / \int_{-1}^0 f_i^h(x_-, n) dx. \quad (27)$$

3. CHARMED AND BEAUTY HADRON PRODUCTION ON NUCLEON TARGET WITH ACCOUNT FOR LOW ENERGY CORRECTIONS

It is well known that perturbative QCD taking into account leading order ($\sim \alpha_s^2$) and next-to-leading order ($\sim \alpha_s^2$) contributions describes quite well the total cross section of heavy flavour production on nucleon targets. However there is a serious problem to reproduce simultaneously the experimental cross sections of D -mesons [16] and Λ_c 's [17] as well as the shapes of their x_F -distributions. In particular, the Parton Fusion Model

[18] assumes that the produced charmed quarks fragment into hadrons thus transferring them some fraction of their momentum and cannot recombine with valence quarks because of the large rapidity gap between charmed and valence quarks. This model predicts the same x_F -distribution for favoured and unfavoured D -mesons in disagreement with data [16,19]. Taking into account the intrinsic charm contribution [20] allows one [21] to describe the x_F -spectra of D -mesons as well as the shape of the Λ_c spectrum. However the Λ_c spectrum at moderate x_F becomes more than two orders of magnitude smaller than the experimental data [17].

QGSM does not have so large problems to describe the data [16,17] on D and Λ_c production [12]. The largest difference is not greater than 2–3 times, which is not very bad keeping in mind the normalization uncertainties. The results of three sets of calculations, without any corrections (QGSMA), with the corrections (25) (QGSMB) and with the corrections (26), (27) (QGSMC), are compared with the experimental data on the cross sections for total charm and for different charmed hadrons in Table 1. The model parameters for these sets are presented in Table 2. Let us note that the value of $\alpha_\psi(0)$ is comparatively well known [6,12,22] whereas the value of $\alpha_Y(0)$ can be changed significantly. For simplicity we use the same parameter values in the cases QGSMA and QGSMB, where the numerical difference of the results is not large.

Let us compare now the results of our calculations with experimental data (Table 1). One can see that the energy dependence of charm production cross section in QGSMB and especially in QGSMC cases is not so strong as in QGSMA. Let us note also that the QGSMC energy dependence is significantly weaker than perturbative QCD predictions if one use modern (i.e., singular at small x) gluon distribution and the same scale values at different energies. In all variants we can see a reasonable agreement with the total cross section of charm production in $p\bar{p}$ collisions at 400 GeV/c [16] and 800 GeV/c [23]. In the case of $Spp\bar{S}$ energy [24], the experimental errors are too large for excluding any variants. In the cases of QGSMA and QGSMB the calculated cross section for D^0 and D^+ production seems to be too small whereas the cross section of $\overline{D^0}$ production is too large. The reasons for this large difference in the calculated values of $\sigma(D)$ and $\sigma(\overline{D})$ are the large values of the parameters a_1 and a_2 in Eq.(8) which is connected with our wish to obtain a comparatively large value of $\sigma(\Lambda_c)$ at $\sqrt{s} = 62$ GeV. Correspondingly the cross section of Λ_c production at 400 GeV/c [16] is also too large. In the case of QGSMC the parameter a_0 can not be taken significantly smaller than the used value to avoid too small a cross section at $\sqrt{s} = 630$ GeV. So the values of a_1 and a_2 can not be taken so large as in the other cases. As a result the D^0 and D^+ cross sections are larger whereas $\sigma(\Lambda_c)$ and $\sigma(\overline{D})$ are closer to the experimental data. Let us remark also the large difference between old [23] and new [25,26] data on D -meson production at 800 GeV/c.

The shapes of the inclusive spectra of D -mesons do not differ significantly with those of [12] as one can see in Fig. 2.

In the case of beauty hadron production we do not have enough data to fix the

parameters of the fragmentation functions. So we use the same fragmentation functions as for charm production with parameters b_i (which are also presented in Table 2) instead of a_i in Eqs. (12)–(21). Namely for B^0 production we use the same fragmentation function as for D^+ , for B^- as for D^0 , for \bar{B}^0 as for D^- , for B^+ as for \bar{D}^0 and for Λ_b as for Λ_c .

The existing experimental point on the total beauty production cross section at $\sqrt{s} = 630$ GeV [27] allow us to fix the parameter b_0 . The values of b_1 and b_2 as well as b_{01} and b_{02} can be estimated from the condition that the cross section of Λ_c production should be (at not very high energy) slightly smaller than the difference of antibeauty and beauty production cross section (including the case of a nuclear target). Naturally the low energy corrections are more important in the case of beauty production and the difference in the predicted energy dependence between the three variants is larger, as one can see in Table 3. Actually we normalize the beauty production cross section at $\sqrt{s} = 630$ GeV using the experimental point [27] and obtain very different predictions for low energy πp collisions. The variants QGSMA and QGSMB predict the last cross section to be very small compared to the data [28, 29] and the variant QGSMC predicts it to be slightly too large. In the case of beauty production in pp collisions at 800 GeV/c [30] the data are in agreement with QGSMA and QGSMB and in strong disagreement with QGSMC. However in Refs. [28–30] nuclear targets were used and the values presented in Table 3 for nucleon targets are the results of a linear extrapolation. So the experimental values possibly can be increased if the A -dependence of beauty production is weaker than A^1 .

Our predictions for beauty production in pp interactions at $\sqrt{s} = 39$ GeV (HERA–B energy) are presented in Table 4. They are in reasonable agreement with the results of the similar calculations of Ref. [13], where the cross section for beauty production was equal to 0.01–0.1 μb depending on the parameters.

4. CHARM AND BEAUTY PRODUCTION ON NUCLEAR TARGETS

The models based on the DTU approach allow one to calculate the inclusive spectra of secondaries produced on nuclear targets [31–34] without new phenomenological parameters. In multiple scattering theory a hadron–nucleus interaction can be considered as a superposition of interactions with a different number of separated nucleons. In the QGSM we account for the possibility of multipomeron interaction in every NN blob [10,34]. One cut pomeron connects a valence quark–diquark pair of the beam nucleon with a quark–diquark pair of a target nucleon. All other pomerons connect sea quark–antiquark pairs of the incident nucleon with valence quark–diquark pairs or sea quark–antiquark pairs of the target nucleons, see Fig. 3. To account for that in our calculation of quark and diquark distributions in the beam nucleon the value of n in Eqs. (5)–(10) is equal to the total number of cutted pomerons in the nucleon–nucleus

interaction, and in the same distributions for a target nucleon the corresponding value of n is equal to the number of pomerons connected with a given nucleon. It provides the asymmetry of the inclusive spectra of secondaries produced on nuclear targets in comparison with a nucleon–nucleon interaction. We assume that the secondaries are produced independently in every shower and their formation zone is large in comparison with the nuclear radius. The contribution of intranuclear cascade to the spectra of secondaries, as well as the Fermi motion of target nucleons, is neglected.

A detailed description of light flavour hadron yields from nuclear targets in the QGSM was presented in Refs. [10,34]. Now we use the same probability of interaction with a given number of target nucleons and consider only the cross sections and the spectra of beauty hadrons.

In the case of QGSMa the charm and beauty cross section in pA collisions has a A^α –dependence with very small α [10]. It is a consequence of the very strong energy dependence of heavy flavour production cross section at comparatively small energies. The initial energy is divided between several cut pomerons so the effective energy of every shower decreases and the corresponding contribution to charm and beauty production cross section is small. So really only the interaction with one target nucleon gives the main contribution to the production cross section in QGSMa. In the case of QGSMb we have approximately the same behaviour because the corrections are comparatively small. However in the case of corrections (26), (27) the situation changes and in this case (QGSMc) the value of α becomes closer to unity (see Table 5, where we present the calculated values of α for the total charm and beauty production cross section in the interval $A = 1 \div 208$).

The predictions of QGSMc for the inclusive spectra of B –mesons and Λ_b ’s produced in pp and pW collisions at $\sqrt{s} = 39$ GeV are presented in Fig. 4. As expected, the cross section of all B –mesons decrease with x_F faster than that of Λ_b ’s. The yields from a nucleus target are larger at small x_F and smaller at large x_F , as usual. Some difference in the nuclear effects for B –mesons and Λ_b ’s can be explained by the diffusion of the last ones from the nuclear fragmentation region to the central region as a consequence of the comparatively small energy.

5. MONTE CARLO RESULTS

In this Section we are going to present the results on beauty production obtained with a QGSM–based Monte Carlo code (a detailed description can be found in Ref. [35]). This Monte Carlo model describes hadron–hadron, hadron–nucleus and nucleus–nucleus collisions on the same footing, at the partonic level. The nuclear parton wave function is constructed as a convolution of parton distributions of individual nucleons with the distribution of nucleons inside the nucleus. The position of each nucleon is

taken to be described by the Woods–Saxon density:

$$\rho(r) = \rho_0 / (1 + \exp[(r - r_0)/a]) , \quad (28)$$

with

$$r_0 = 1.19A^{1/3} + 1.61A^{-1/3} \text{ fm}, \quad a = 0.54 \text{ fm}. \quad (29)$$

To take the Fermi motion of nucleons into account we generate a Fermi momentum p for each nucleon uniformly distributed in the range $0 < p < p_F$, where p_F is the maximum Fermi nucleon momentum:

$$p_F = (3\pi^2)^{1/3} h \rho^{1/3}(r) , \quad (30)$$

with $h = 0.197 \text{ fm GeV/c}$. Isotropical angular distribution is assumed in both the coordinate and momentum spaces.

As to the parton distribution for individual nucleons this is taken to be the same as for NN collisions. In particular, the distribution in the number of partons in a nucleon, which is directly connected with the value of the multipomeron vertices in the reggeon theory ([36]), is taken poissonian:

$$w_N = \exp(-g(s)) g^N(s) / N! , \quad (31)$$

corresponding to the eikonal picture. The mean number of partons in each nucleon, $g(s) = g_0 s^\Delta$, is a function of the center of mass energy \sqrt{s} . We use $g_0 = 3.0$ and $\Delta = 0.09$.

The parton distribution in impact parameter (relative to the center of the corresponding nucleon) is taken to be gaussian, in accordance with the Pomeron picture of strong interactions:

$$F(b_p) = (4\pi\lambda)^{-1} \exp(-b_p^2/4\lambda) , \quad (32)$$

with the radius depending on the initial nucleon energy. For a projectile or target nucleon, $\lambda = R^2 + \alpha' \ln \sqrt{s}$, where $\alpha' = 0.01 \text{ fm}^2$ and $R^2 = 0.15 \text{ fm}^2$.

A hadron or nucleus collision is assumed to be the interaction between partons from the projectile and target. A parton from the projectile can interact with one from the target if they lie in impact parameter space within an area determined by the parton–parton cross section, which has been assumed energy independent, $\sigma_p = 3.5 \text{ mb}$.

In this way the number of inelastic collisions is determined and the inelastic cross section is calculated (an elastic event is one with no partons close enough in impact parameter space).

Now, opposite to Ref. [35] (where each inelastic collision could be a hard or a soft one with a probability $w(s)$), each inelastic collision is taken to be a hard gluon–gluon one. For simulating these gg collisions the PYTHIA program ([37]) is used. Only $gg \rightarrow gg$, $gg \rightarrow q\bar{q}$ and $gg \rightarrow Q\bar{Q}$ collisions, with q and Q light and heavy flavours respectively,

are considered. In our calculations we have used the EHLQ set 1 structure functions ([38]), a $K = 2.0$ factor and a $p_t^{\min} = 2.3$ GeV/c.

Using this model we have computed the x_F – and p_t –distributions of particles with beauty in pp and pW collisions at $\sqrt{s} = 39$ GeV (Figs. 5 and 6). The number of generated events is 600000 for pp and 400000 for pW collisions. Also in the last column of Table 5 we present the Monte Carlo results for the A –dependence of charm and beauty cross sections.

6. CONCLUSIONS

In this paper we have presented results of QGSM for heavy flavour production at different energies. Three variants of QGSM have been described, which try to take into account corrections which are important at not very high energies. Besides, results of a Monte Carlo code [35] for production of beauty particles at HERA–B energy have been shown.

We can see that the three variants of QGSM describe reasonably most of the existing data on charmed hadron production. Some contradictions are connected with the significant differences of different sets of experiment data. For example, the cross section of Λ_c production measured in Ref. [16] is very small in comparison with the data of Ref. [17]. If the Λ_c production cross section is really so small the difference in \bar{D} and D production cross sections could be obtained smaller by decreasing the parameters a_1 and a_2 in Eqs. (13), (16) and (17).

In the case of beauty production at $\sqrt{s} = 39$ GeV the model cannot describe simultaneously the data obtained with proton and pion beams [28–30]. As one can see in these experimental papers, perturbative QCD also can not describe them with the same parameters (QCD scale and quark masses). In our case we can describe the proton beam data in the cases of QGSMA and QGSMB and the pion beam data are in reasonable agreement with QGSMC. A possible explanation of such situation can be the assumed A –dependence of beauty production, which could be weaker than A^1 . However this would be in disagreement with the direct measurement of the A –dependence of D –meson production [26] where $\alpha = 1.02 \pm 0.03 \pm 0.02$.

So the variants QGSMA and QGSMB predict the beauty production cross section in pp collisions at $\sqrt{s} = 39$ GeV equal to $5 \div 7$ nb in agreement with data [30] and in this case they cannot describe the data of beauty production by pion beams [28, 29]. The variant QGSMC is in reasonable agreement with the data [29], gives slightly too large cross sections in comparison with the data [28] and predicts the cross section of beauty production in pp collisions at $\sqrt{s} = 39$ GeV equal to $0.2 \div 0.3$ μb with an A –dependence $\sim A^{0.99}$. The A –dependence obtained in the Monte Carlo calculations is $A^{0.89}$, closer the the variant QGSMC than to QGSMA or QGSMB.

We are grateful to R. Rueckl for stimulating discussions. We also thank the Xunta

de Galicia, the Dirección General de Política Científica and the CICYT of Spain for financial support.

References

- [1] P. Nason, S. Dawson and R. K. Ellis, Nucl. Phys. B303 (1988) 607.
- [2] G. Altarelli et al., Nucl. Phys. B308 (1988) 724.
- [3] W. Beenakker et al., Nucl. Phys. B351 (1991) 507.
- [4] M. Mangano, P. Nason and G. Ridolfi, Nucl. Phys. B405 (1993) 507.
- [5] E. L. Berger, Phys. Rev. D37 (1988) 1810.
- [6] A. B. Kaidalov and O. I. Piskunova, Yad. Fiz. 43 (1986) 1545.
- [7] A. B. Kaidalov and K. A. Ter-Martirosyan, Yad. Fiz. 39 (1984) 1545; 40 (1984) 211.
- [8] A. B. Kaidalov and O. I. Piskunova, Yad. Fiz. 41 (1985) 1278.
- [9] Yu. M. Shabelski, Yad. Fiz. 44 (1986) 186.
- [10] Yu. M. Shabelski, Z. Phys. C38 (1988) 569.
- [11] V. A. Abramovski, V. N. Gribov and O. V. Kancheli, Yad. Fiz. 18 (1973) 595.
- [12] Yu. M. Shabelski, Yad. Fiz. 55 (1992) 2227.
- [13] O. I. Piskunova, Yad. Fiz. 56 (1993) 176; 57 (1994) 538.
- [14] T. Lohse et al., HERA-B Proposal, DESY-PRC 94/02 (1994).
- [15] K. A. Ter-Martirosyan, Phys. Lett. 44B (1973) 377.
- [16] M. Aguilar-Benítez et al., Z. Phys. C40 (1988) 321.
- [17] G. Bari et al., Nuovo Cim. 104A (1991) 571.
- [18] S. Banerjee and S. N. Ganguli, Phys. Rev. D33 (1986) 1278.
- [19] M. Aguilar-Benítez et al., Phys. Lett. 161B (1985) 400.
- [20] S. J. Brodsky et al., Phys. Lett. 93B (1980) 451; S. J. Brodsky, C. Peterson and N. Sakai, Phys. Rev. D23 (1981) 2745.
- [21] R. Vogt, S. J. Brodsky and P. Hoyer, Nucl. Phys. B383 (1992) 643.
- [22] G. L. Balayan, A. G. Oganessian and A. Yu. Khodjamirian, Yad. Fiz. 49 (1989) 682; A. G. Oganessian and A. Yu. Khodjamirian, Yad. Fiz. 56 (1993) 1720.
- [23] R. Ammar et al., Phys. Lett. B183 (1987) 110.

- [24] O. Botner et al., *Phys. Lett.* B236 (1990) 488.
- [25] K. Kodama et al., *Phys. Lett.* B263 (1991) 573.
- [26] M. J. Leitch et al., *Phys. Rev. Lett.* 72(1994) 2542.
- [27] C. Albajar et al., *Phys. Lett.* B256 (1991) 121.
- [28] K. Kodama et al., *Phys. Lett.* B303 (1993) 359.
- [29] R. Jesik et al., *Phys. Rev. Lett.* 74 (1995) 495.
- [30] D. M. Jansen et al., *Phys. Rev. Lett.* 74 (1995) 3118.
- [31] A. Capella, U. P. Sukhatme, C.-I. Tan and J. Tran Thanh Van, *Phys. Rep.* 236 (1994) 225.
- [32] W. Q. Chao et al., *Phys. Rev. Lett.* 44 (1980) 518.
- [33] J. Ranft and S. Z. Ritter, *Z. Phys.* C20 (1983) 347.
- [34] A. B. Kaidalov, K. A. Ter-Martirosyan and Yu. M. Shabelski, *Yad. Fiz.* 43 (1986) 1282.
- [35] N. S. Amelin, H. Stöcker, W. Greiner, N. Armesto, M. A. Braun and C. Pajares, Santiago preprint US-FT/1-94 (to be published in *Phys. Rev. C*).
- [36] V. A. Abramovski, E. V. Gedalin, E. G. Gurvich and O. V. Kancheli, *Sov. J. Nucl. Phys.* 53 (1991) 271.
- [37] T. Sjöstrand, *Comput. Phys. Commun.* 39 (1986) 347; CERN preprint CERN-TH 6488 (1992); T. Sjöstrand and H.-U. Bengtsson, *Comput. Phys. Commun.* 43 (1987) 367.
- [38] E. Eichten, I. Hinchliffe, K. Lane and C. Quigg, *Rev. Mod. Phys.* 56 (1984) 579.

Table 1

Comparison of the experimental cross sections (in μb) of different charmed hadrons produced in pp and πp interactions with the results of our QGSM calculations. In the case of πp collisions, the cross sections are given only in the region $x_F > 0$ (i.e., in the outgoing π hemisphere).

Reaction, \sqrt{s}	Experiment	QGSMA	QGSMB	QGSMC
$\pi^- p \rightarrow D^+/D^-, 26 \text{ GeV}$	5.7 ± 1.6	9.7	10.7	11.2
$\pi^- p \rightarrow D^0/\bar{D}^0, 26 \text{ GeV}$	10.1 ± 2.2	6.3	7.1	10.3
$pp \rightarrow c\bar{c}, 27 \text{ GeV}$	$14\text{--}23$	28	33	30
$pp \rightarrow D^+/D^-, 27 \text{ GeV}$	11.9 ± 1.5	12	14.2	23.9
$pp \rightarrow D^0/\bar{D}^0, 27 \text{ GeV}$	18.3 ± 2.5	23.4	27.4	26.6
$pp \rightarrow D^0, 27 \text{ GeV}$	10.5 ± 1.9	3.7	4.4	10.5
$pp \rightarrow \bar{D}^0, 27 \text{ GeV}$	7.9 ± 1.5	19.7	23	16.1
$pp \rightarrow D^+, 27 \text{ GeV}$	5.7 ± 1.1	3.7	4.4	10.5
$pp \rightarrow D^-, 27 \text{ GeV}$	6.2 ± 1.1	8.3	9.8	13.4
$pp \rightarrow \Lambda_c, 27 \text{ GeV}$	$< 6.1 (\Lambda_c/D)$	14.6	14.6	7.3
	$< 15 (\Lambda_c/\bar{\Lambda}_c)$	—	—	—
$pp \rightarrow c\bar{c}, 39 \text{ GeV}$	$29\text{--}55$	47	52	41
$pp \rightarrow D^+/D^-, 39 \text{ GeV}$	33 ± 7	25	27	34
$pp \rightarrow D^0/\bar{D}^0, 39 \text{ GeV}$	26_{-13}^{+21}	40	44	38
$pp \rightarrow D^0/\bar{D}^0, 39 \text{ GeV}$	$17.7 \pm 0.9 \pm 3.4$	—	—	—
$pp \rightarrow D^0, 39 \text{ GeV}$	$38 \pm 3 \pm 13$	6.5	10	15.5
$pp \rightarrow D^+, 39 \text{ GeV}$	$38 \pm 9 \pm 14$	6.5	10	15.5
$pp \rightarrow \Lambda_c, 62 \text{ GeV}$	$(40 \pm 18) \div (204 \pm 91)$	19	19	8.9
$pp \rightarrow c\bar{c}, 630 \text{ GeV}$	$680 \pm 560 \pm 250 \pm 210$	660	660	415

Table 2

The values of the parameters used for the calculations of charm and beauty production in QGSM.

Parameter	QGSMA	QGSMB	QGSMC
$\alpha_\psi(0)$	-2	-2	-2
a_0	0.024	0.024	0.02
a_1	10	10	0
a_2	50	50	16
a_{01}	0.011	0.011	0.007
a_{02}	0.005	.005	0.0025
$\alpha_Y(0)$	-8	-8	-8
b_0	0.011	0.011	0.0055
b_1	5	5	6
b_2	25	25	40
b_{01}	0.005	0.005	0.0015
b_{02}	0.0004	.0004	0.0018

Table 3

Comparison of the experimental cross sections of beauty production in pp and πp interactions with the results of our present QGSM calculations.

Reaction, \sqrt{s}	Experiment	QGSMA	QGSMB	QGSMC
$\pi^- p \rightarrow b\bar{b}$, 31 GeV	$75 \pm 31 \pm 26$ nb	2.4 nb	2.8 nb	125 nb
$\pi^- p \rightarrow b\bar{b}$, 31 GeV, $x_F > 0$	$47 \pm 19 \pm 14$ nb	0.8 nb	1.0 nb	63 nb
$\pi^- p \rightarrow b\bar{b}$, 34 GeV	$33 \pm 11 \pm 6$ nb	4.7 nb	5.5 nb	154 nb
$pp \rightarrow b\bar{b}$, 39 GeV	$5.7 \pm 1.5 \pm 1.3$ nb	4.8 nb	6.8 nb	270 nb
$pp \rightarrow b\bar{b}$, 630 GeV	$19.3 \pm 7 \pm 9$ μ b	21 μ b	21 μ b	8 μ b

Table 4

Predictions for beauty production in pp interactions at $\sqrt{s} = 39$ GeV. All the cross sections are in nb.

Reaction	QGSMa	QGSMb	QGSMc
$pp \rightarrow b\bar{b}$	4.8	6.8	270
$pp \rightarrow B^+/B^-$	3.9	5.5	220
$pp \rightarrow B^0/\bar{B}^0$	2.1	3	210
$pp \rightarrow \Lambda_b$	1.1	1.1	80

Table 5

Predictions for the A -dependence ($\sigma \sim A^\alpha$) of charm and beauty production on nuclear targets in the interval $A = 1 \div 208$ at $\sqrt{s} = 39$ GeV.

Parameter	QGSMa	QGSMb	QGSMc	Monte Carlo
$\alpha(c\bar{c})$	0.74	0.75	0.85	0.87
$\alpha(b\bar{b})$	0.56	0.57	0.99	0.89

Figure captions

Fig.1. Cylindrical diagram which corresponds to the one-pomeron exchange contribution to elastic pp scattering (a). Its cut which determine the contribution to inelastic pp cross section (b). The diagram which correspond to the cut of three pomerons (c).

Fig.2. Inclusive spectra of all D -mesons produced in pp interactions at 400 GeV/c [16] and its description by QGSMA (solid curve), QGSMB (dashed curve) and QGSMC (dashed-dotted curve). The dotted curve represent the result of Ref. [12].

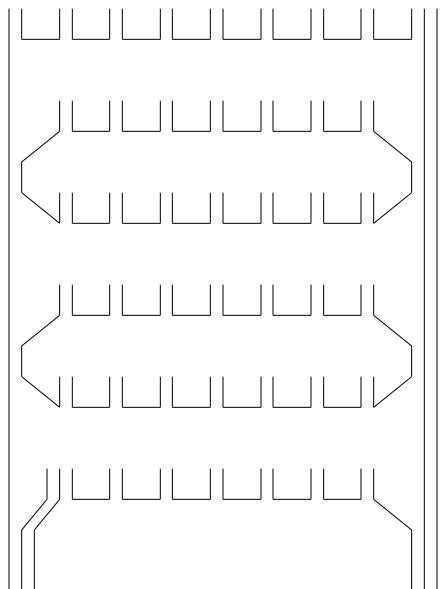
Fig.3. Example of a diagram of interaction of the beam nucleon with two target nucleons.

Fig.4. Spectra of all B -mesons and Λ_b 's at $\sqrt{s} = 39$ GeV for a proton beam on hydrogen (solid curves) and lead (dashed curves) targets using the QGSMC.

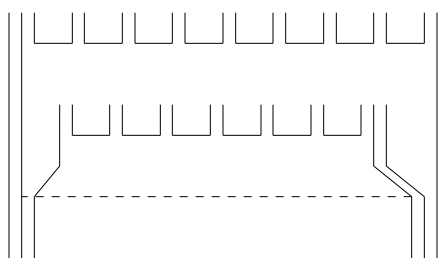
Fig. 5. x_F -distributions (normalized to unity) of beauty particles in: a) pp and b) pW collisions at $\sqrt{s} = 39$ GeV.

Fig. 6. p_t -distributions (normalized to unity) of beauty particles in: a) pp and b) pW collisions at $\sqrt{s} = 39$ GeV.

c



b



a



Fig. 1

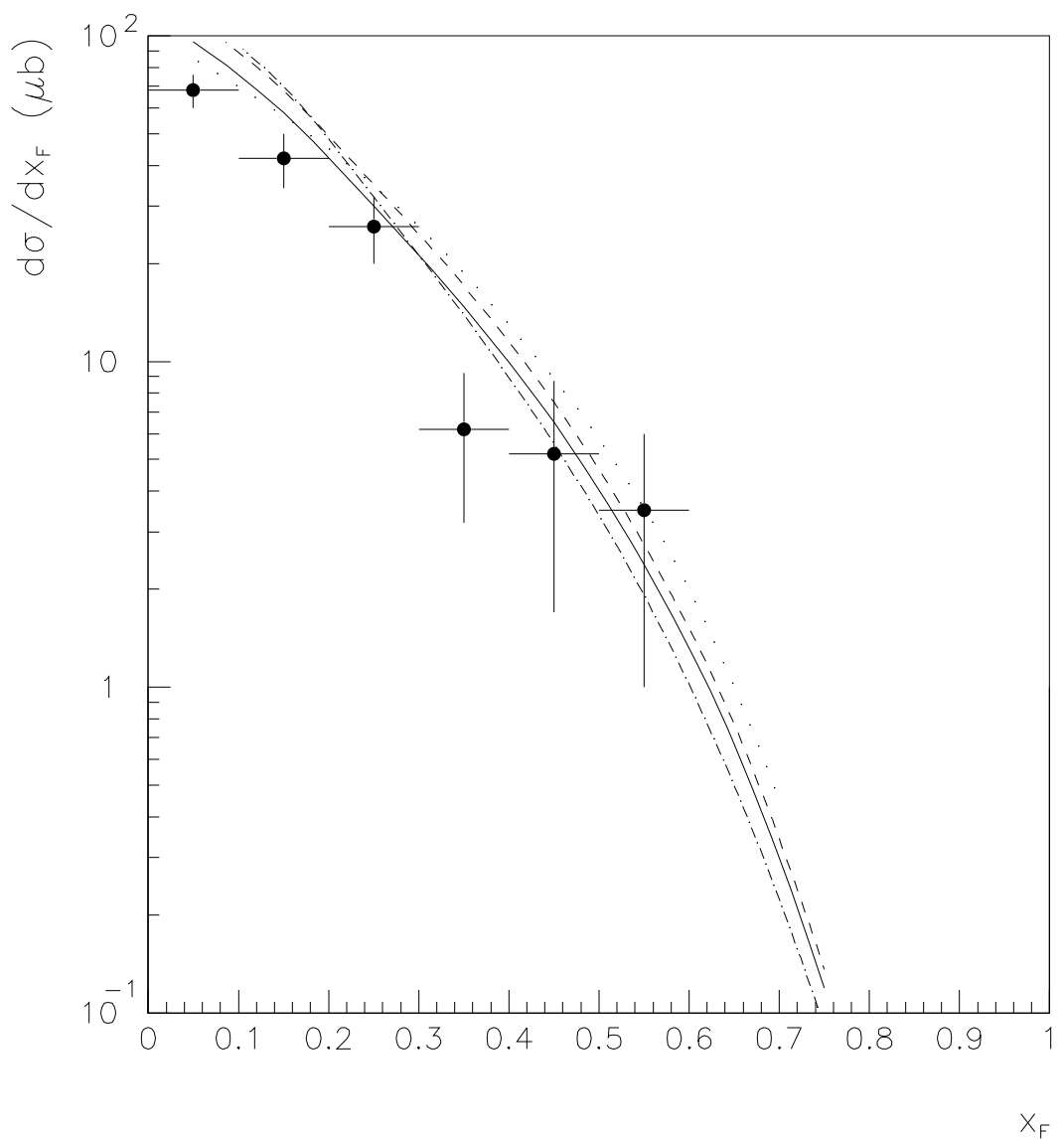


Fig. 2

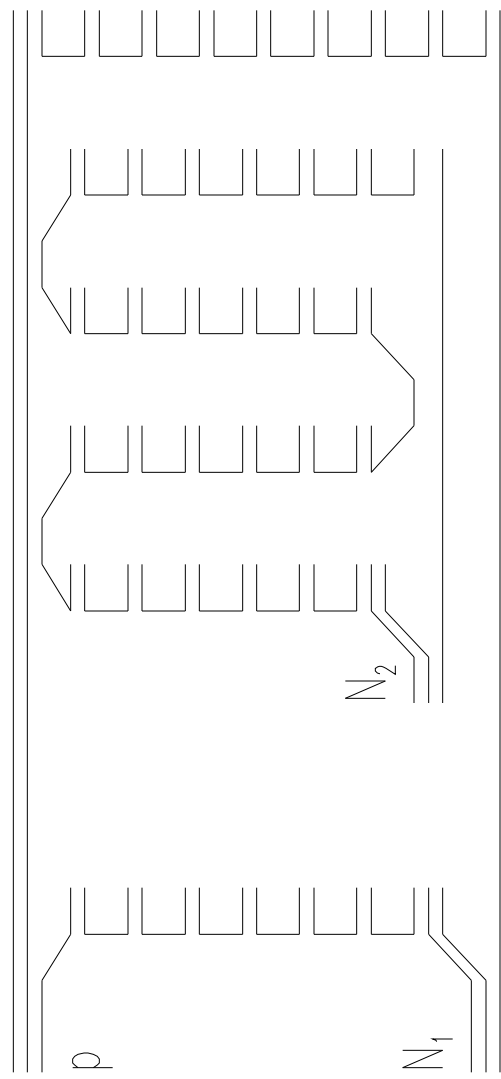


Fig. 3

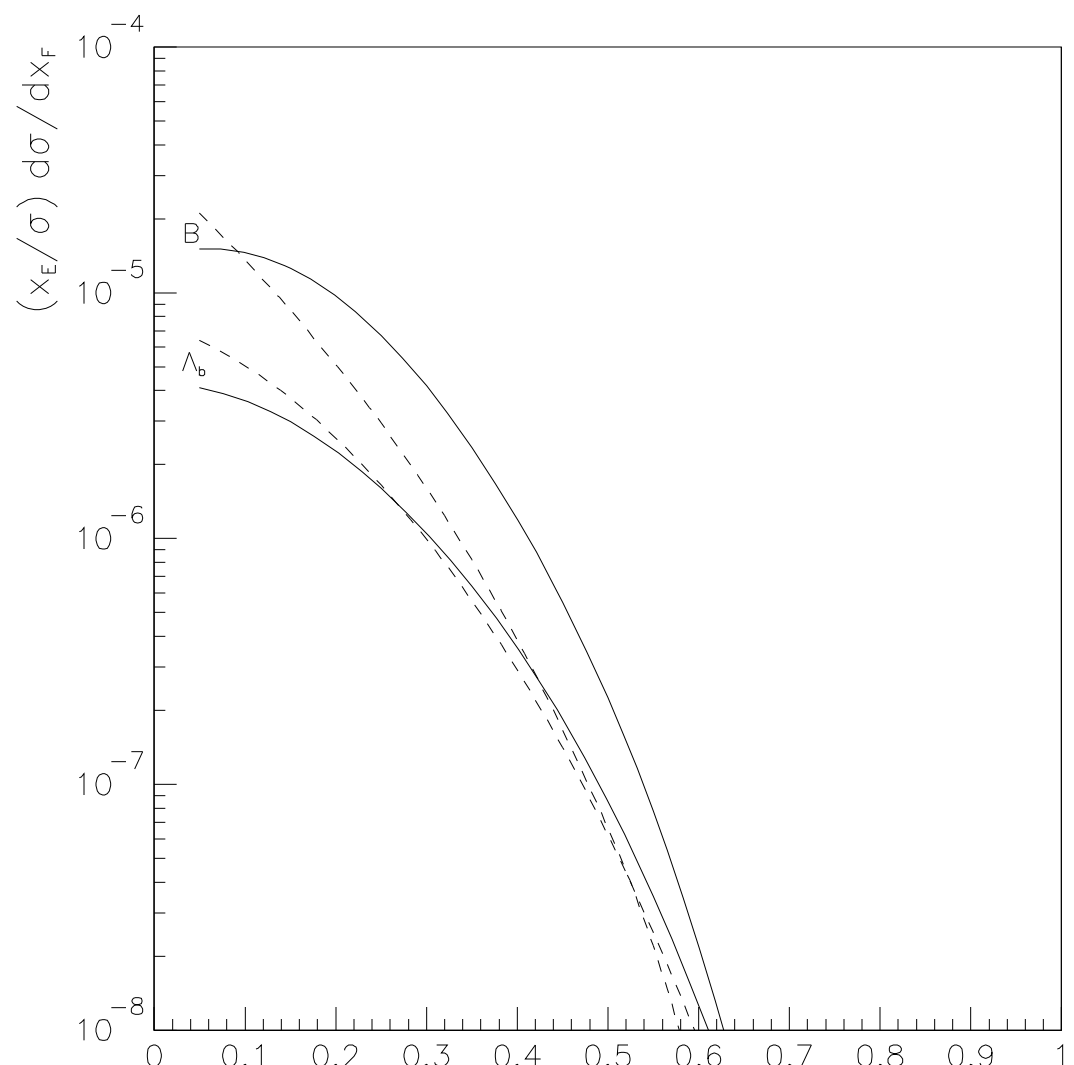


Fig. 4

x_F

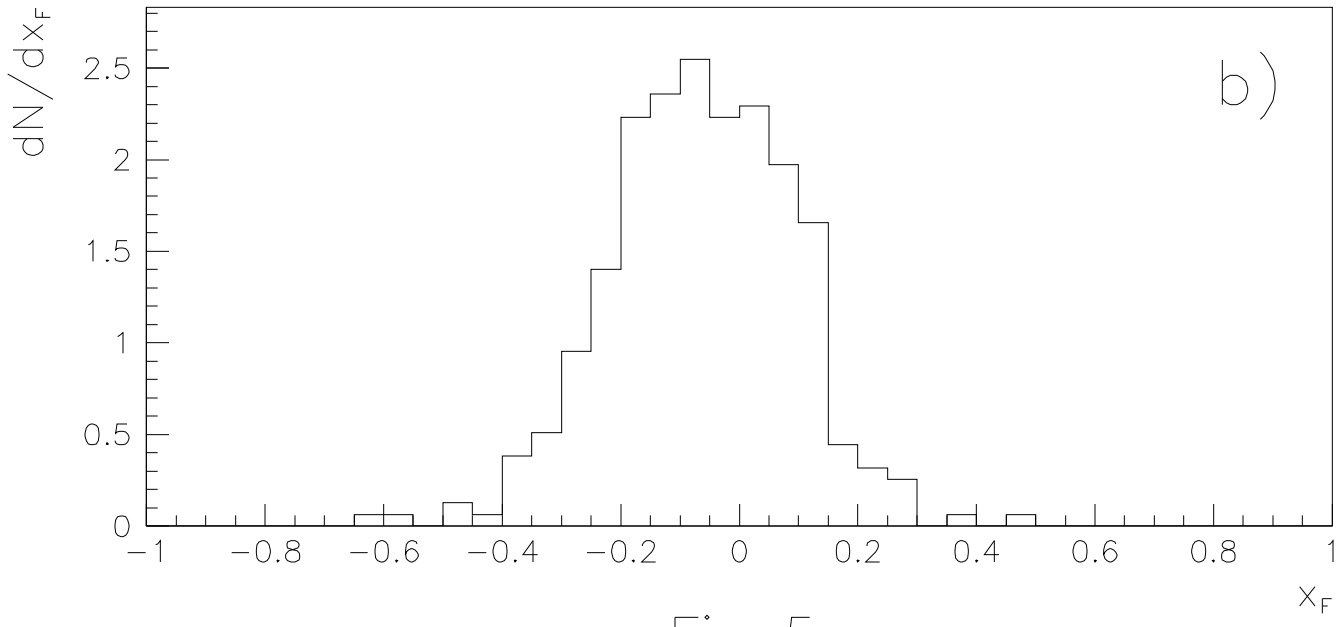
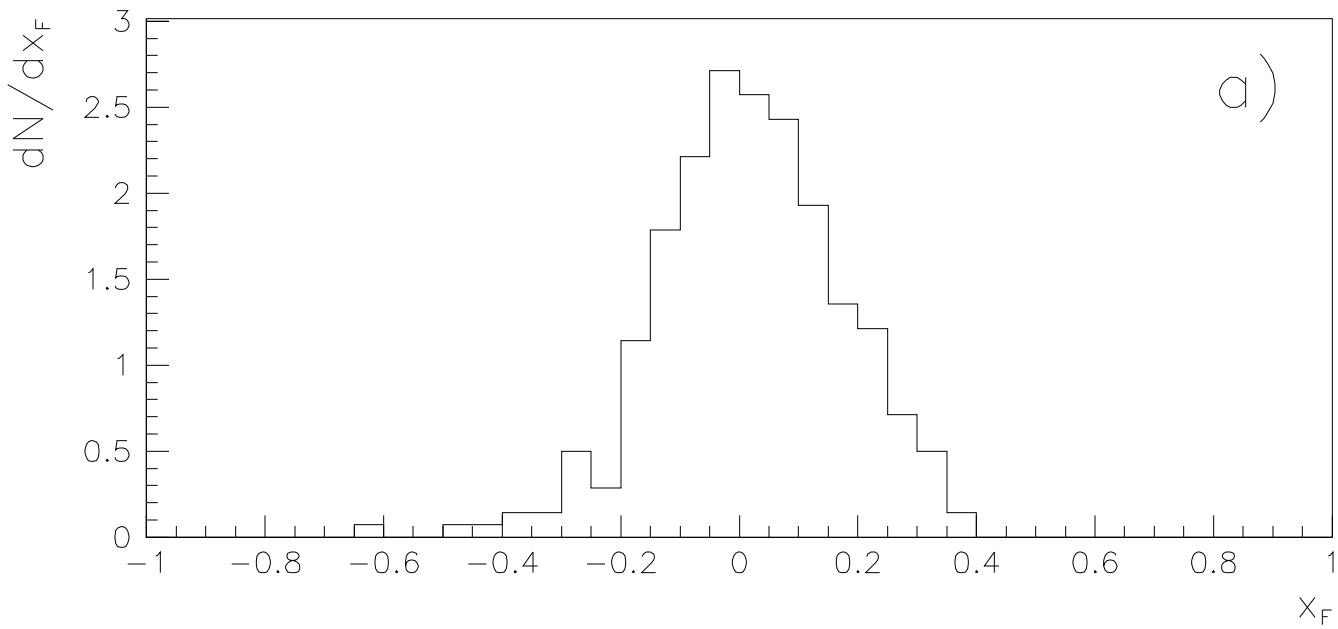


Fig. 5

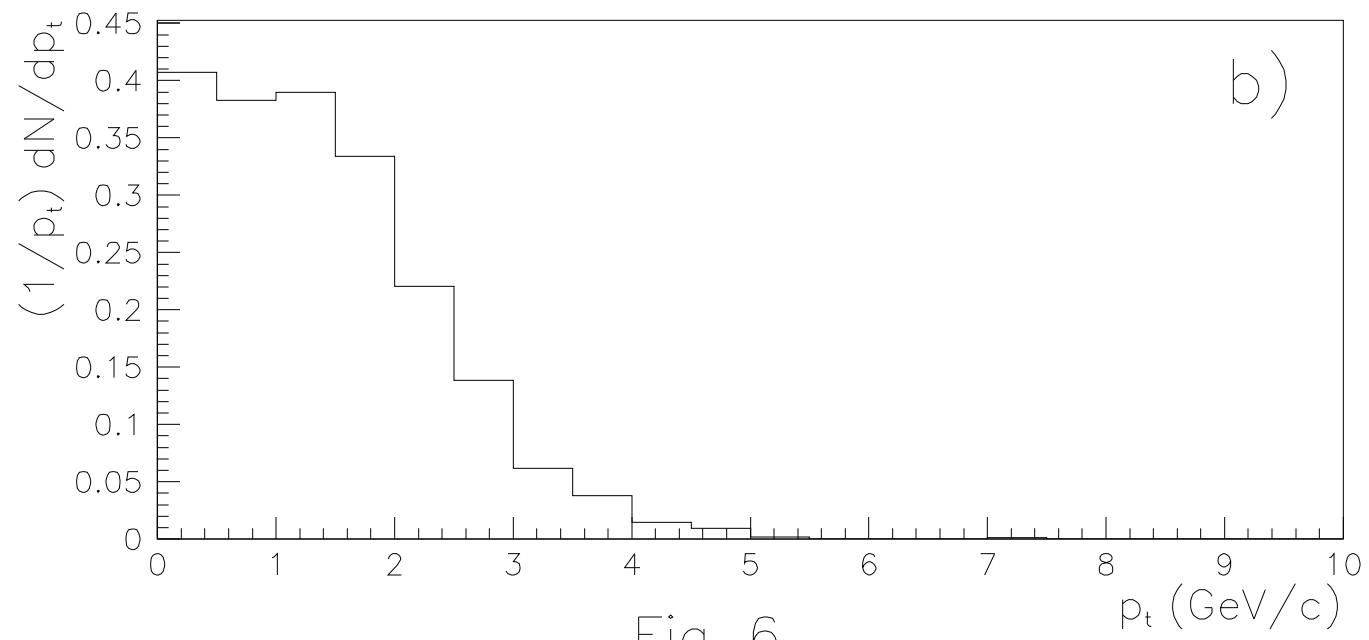
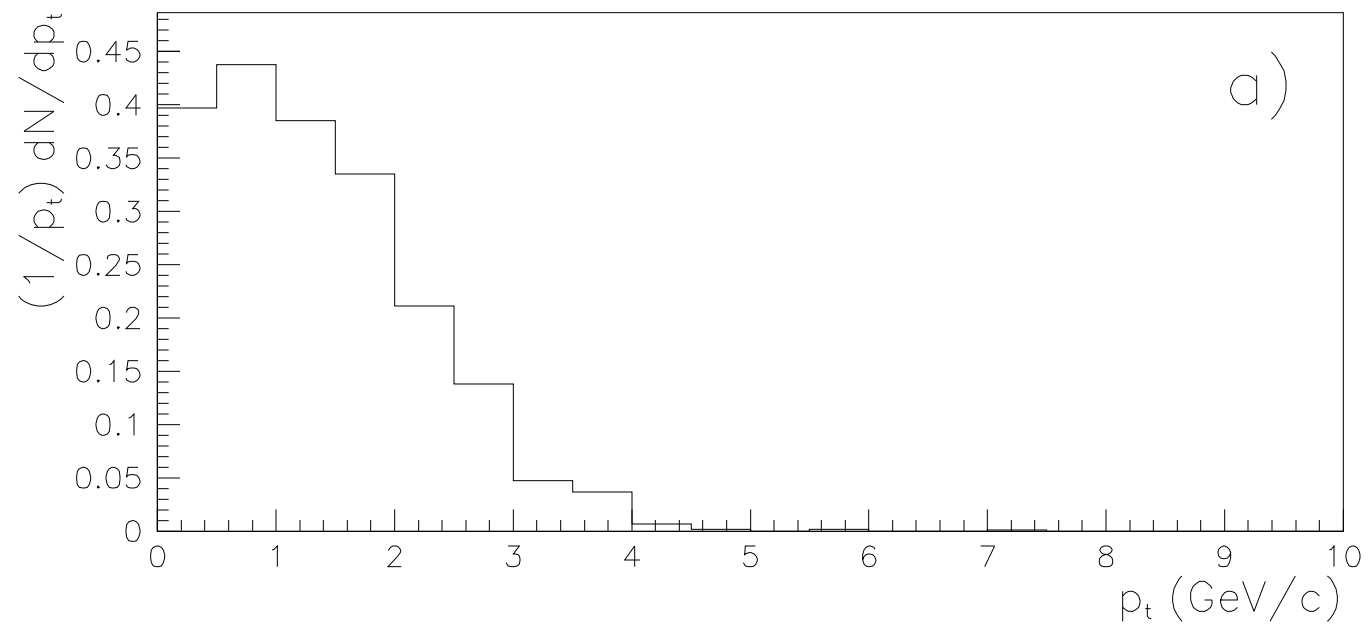


Fig. 6